

Electrical impedance tomography and virtual X-rays

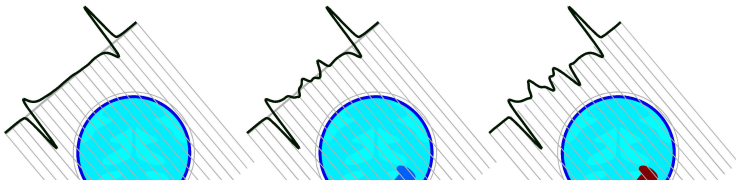
Samuli Siltanen

Department of Mathematics and Statistics
University of Helsinki, Finland
samuli.siltanen@helsinki.fi
www.siltanen-research.net

Tomographic Inverse Problems: Theory and Applications

Mathematisches Forschungsinstitut Oberwolfach

31.1.2019



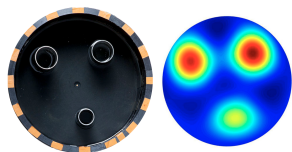
Finnish Centre of Excellence in Inverse Modelling and Imaging 2018-2025



Links to open computational resources

Open EIT datasets:

- [Finnish Inverse Problems Society \(FIPS\) dataset page](#)



Reconstruction algorithms: FIPS Computational Blog

- [The D-bar Method for EIT—Simulated Data](#)
- [The D-bar Method for EIT—Experimental Data](#)

For these slides see: <http://www.siltanen-research.net/talks.html>

Outline

Electrical impedance tomography (EIT)

Complex geometric optics (CGO) solutions, D-bar method

Application of EIT to stroke

Virtual Hybrid Edge Detection (VHED)

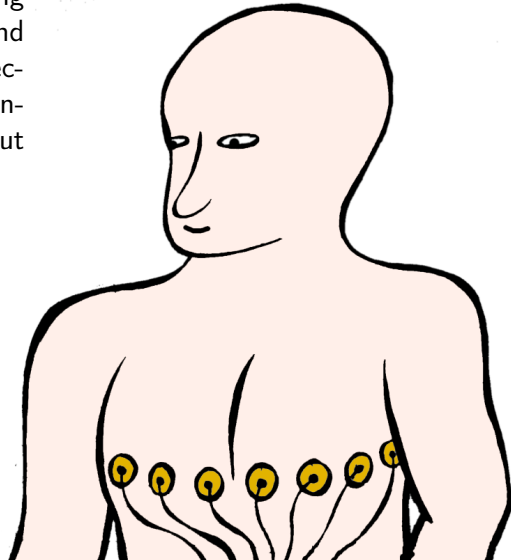
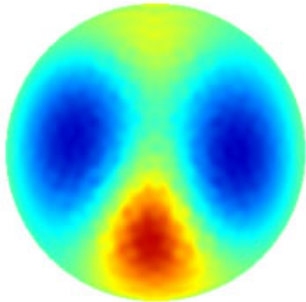
The scattering series

Filtered back-projection theorem

Why machine learning?

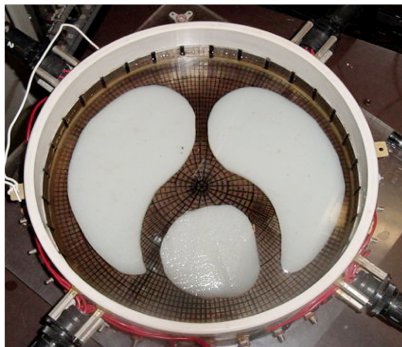
This section concentrates on applications of EIT to chest imaging

Medical applications: monitoring cardiac activity, lung function, and pulmonary perfusion. Also, electrocardiography (ECG) can be enhanced using knowledge about conductivity distribution.

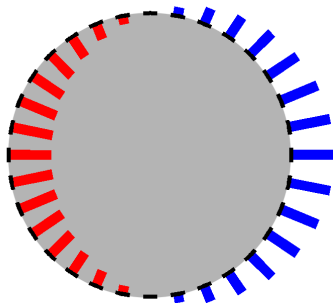


Note that EIT data collection involves applying several current patterns

Saline and agar phantom



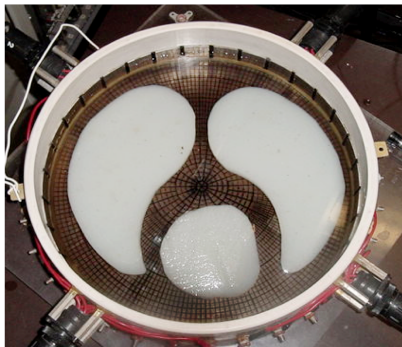
Apply current pattern $\cos \theta$



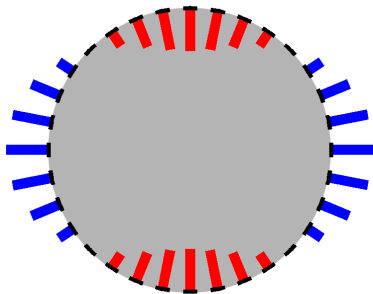
Measure the resulting voltages at the 32 electrodes

Note that EIT data collection involves applying several current patterns

Saline and agar phantom



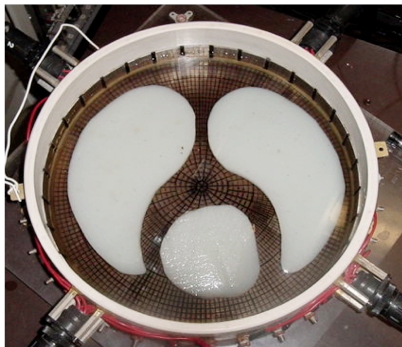
Apply current pattern $\cos 2\theta$



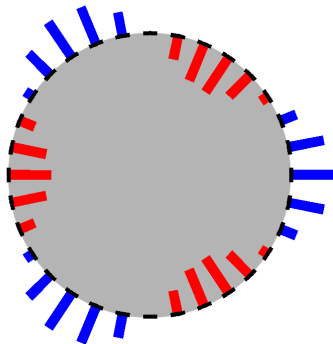
Measure the resulting voltages at the 32 electrodes

Note that EIT data collection involves applying several current patterns

Saline and agar phantom



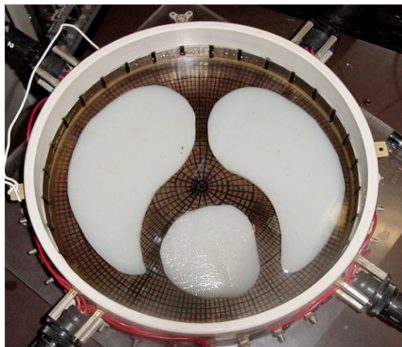
Apply current pattern $\cos 3\theta$



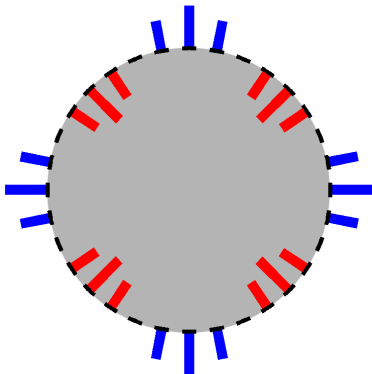
Measure the resulting voltages at the 32 electrodes

Note that EIT data collection involves applying several current patterns

Saline and agar phantom



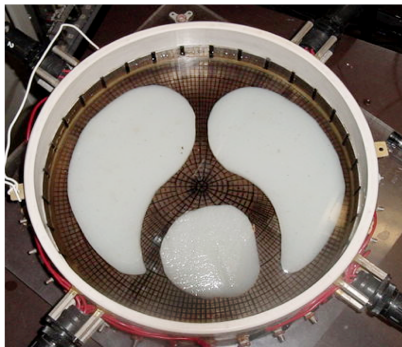
Apply current pattern $\cos 4\theta$



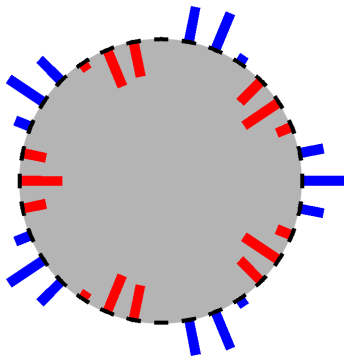
Measure the resulting voltages at the 32 electrodes

Note that EIT data collection involves applying several current patterns

Saline and agar phantom



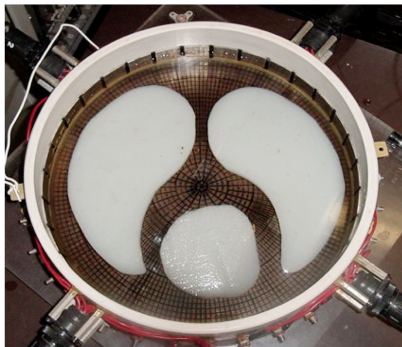
Apply current pattern $\cos 5\theta$



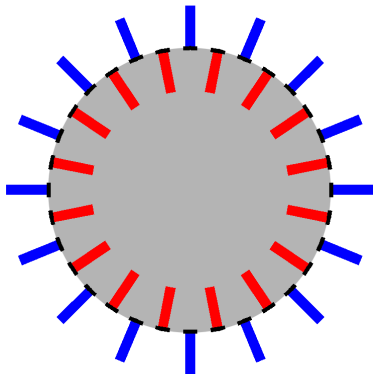
Measure the resulting voltages at the 32 electrodes

Note that EIT data collection involves applying several current patterns

Saline and agar phantom



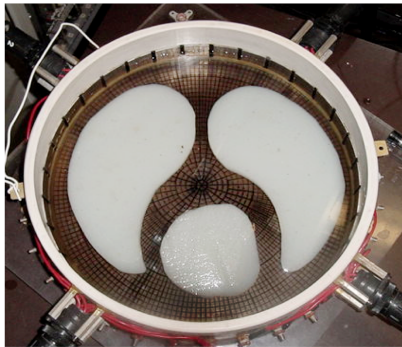
Apply current pattern $\cos 16\theta$



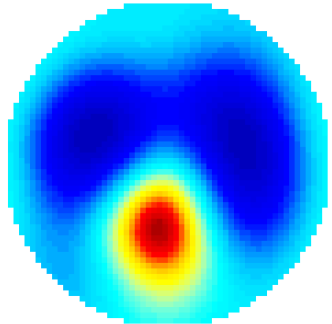
Measure the resulting voltages at the 32 electrodes

The D-bar method works for real EIT data, such as laboratory phantoms and *in vivo* human data

Saline and agar phantom



Reconstruction ($R = 4$)



[Isaacson, Mueller, Newell & S 2004]

[Montoya 2012]

The mathematical model of EIT is the inverse conductivity problem introduced by Calderón

Let $\Omega \subset \mathbb{R}^2$ be the unit disc and let conductivity $\sigma : \Omega \rightarrow \mathbb{R}$ satisfy

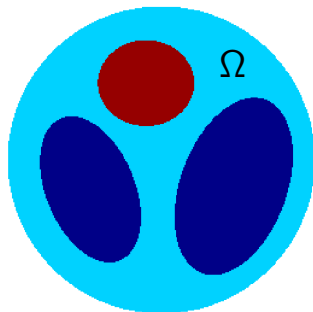
$$0 < M^{-1} \leq \sigma(z) \leq M.$$

Applying voltage f at the boundary $\partial\Omega$ leads to the elliptic PDE

$$\begin{cases} \nabla \cdot \sigma \nabla u &= 0 \text{ in } \Omega, \\ u|_{\partial\Omega} &= f. \end{cases}$$

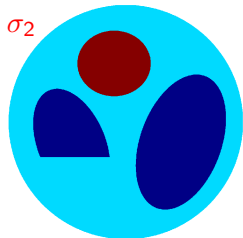
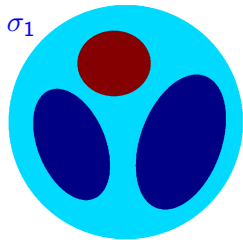
Boundary measurements are modelled by the Dirichlet-to-Neumann map

$$\Lambda_\sigma : f \mapsto \sigma \frac{\partial u}{\partial \vec{n}}|_{\partial\Omega}.$$

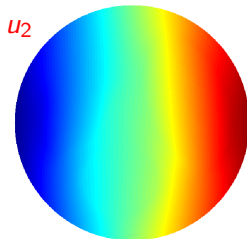
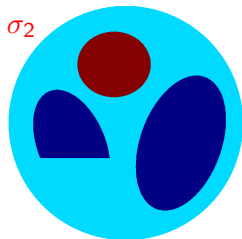
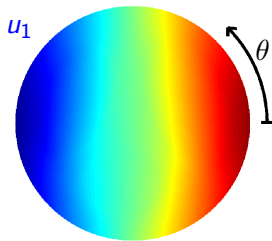
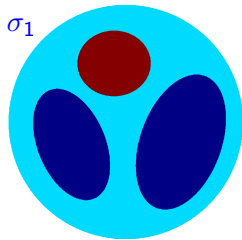


Calderón's problem is to recover σ from the knowledge of Λ_σ . It is a nonlinear and ill-posed inverse problem.

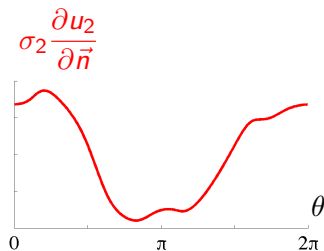
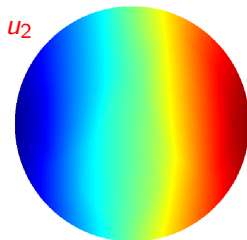
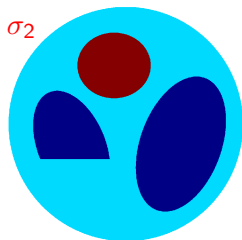
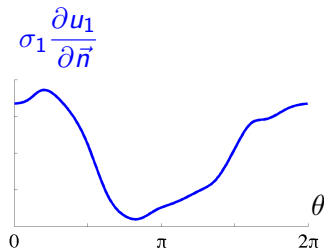
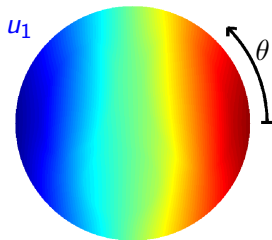
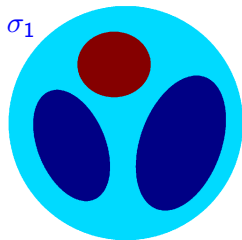
We illustrate the ill-posedness of EIT
using a simulated example



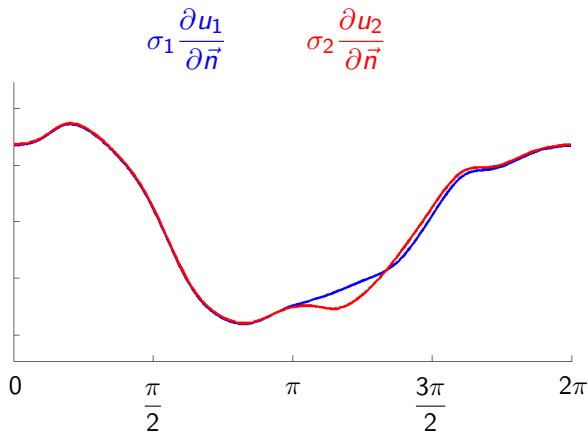
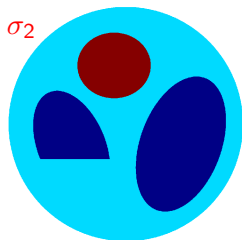
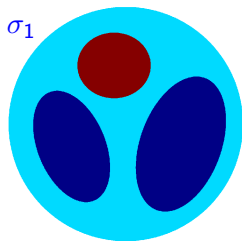
We apply the voltage distribution $f(\theta) = \cos \theta$ at the boundary of the two different phantoms



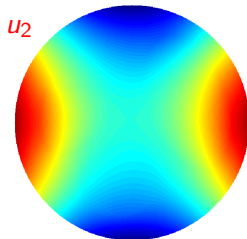
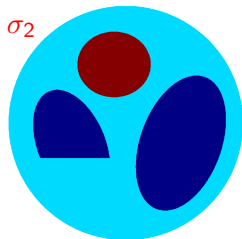
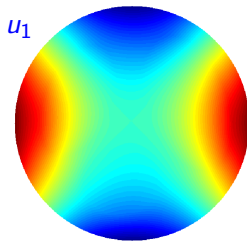
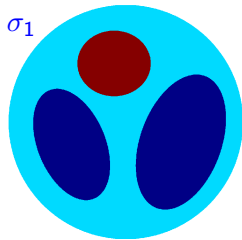
The measurement is the distribution of current through the boundary



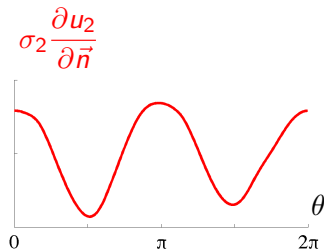
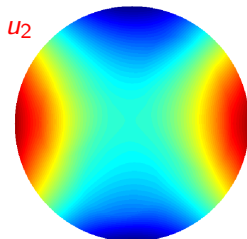
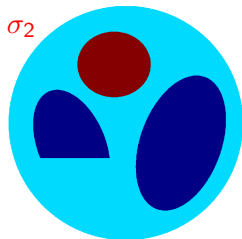
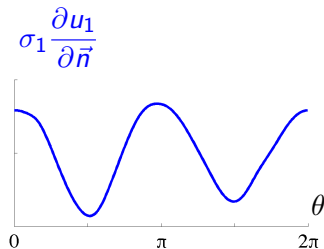
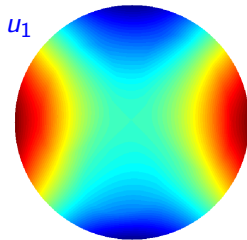
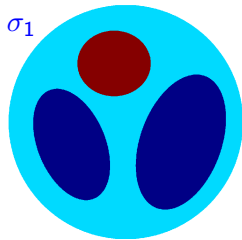
The current data are very similar,
although the conductivities are quite different



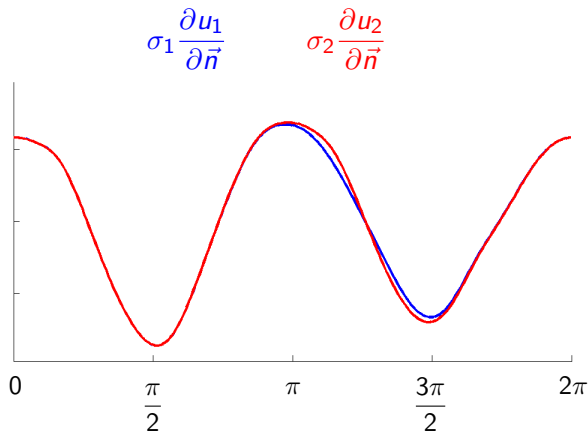
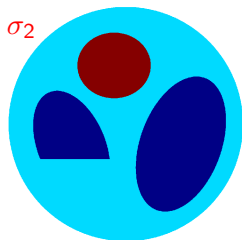
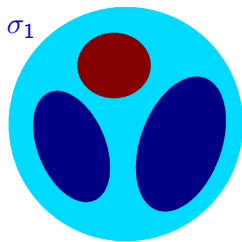
Let us apply the more oscillatory distribution
 $f(\theta) = \cos 2\theta$ of voltage at the boundary



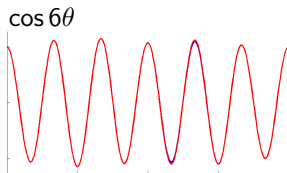
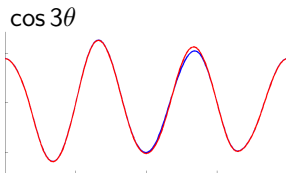
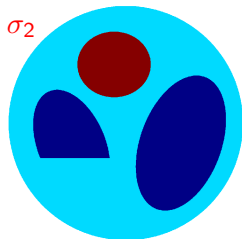
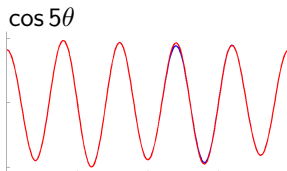
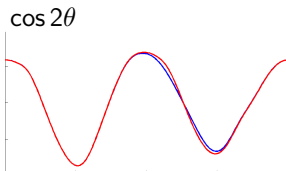
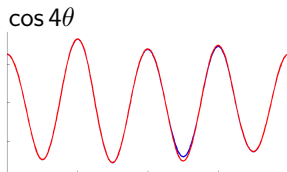
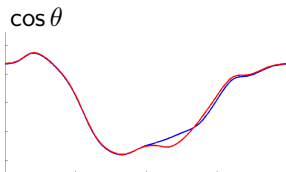
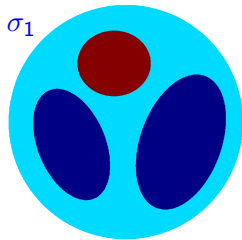
The measurement is again the distribution of current through the boundary



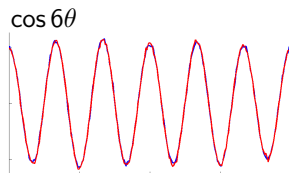
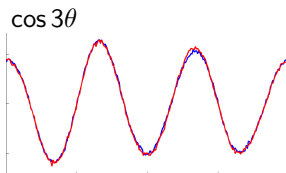
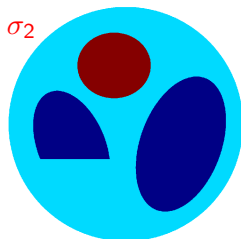
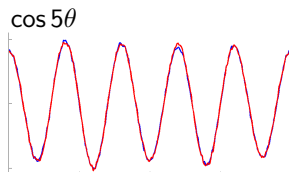
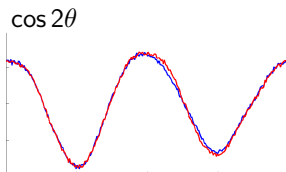
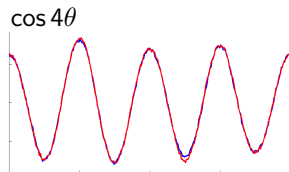
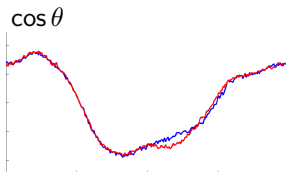
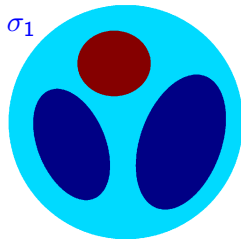
The current distribution measurements
are almost the same



EIT is an ill-posed problem: big differences in conductivity cause only small effect in data



EIT is an ill-posed problem: noise in data causes serious difficulties in interpreting the data



Outline

Electrical impedance tomography (EIT)

Complex geometric optics (CGO) solutions, D-bar method

Application of EIT to stroke

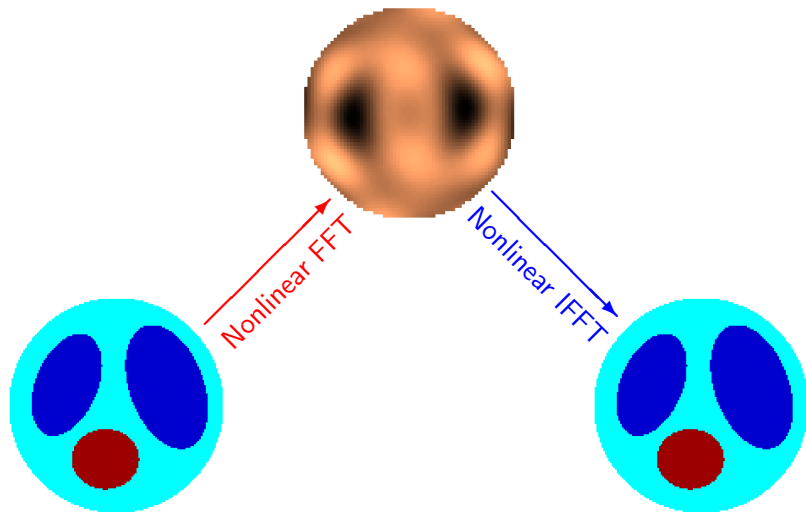
Virtual Hybrid Edge Detection (VHED)

The scattering series

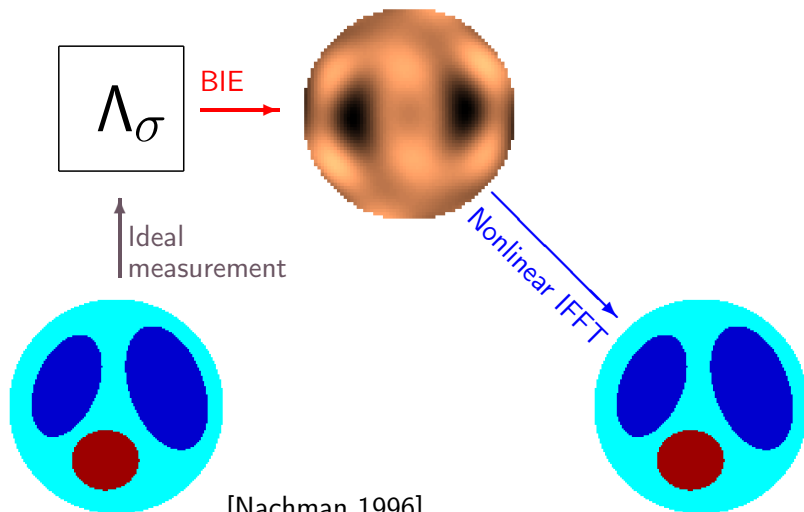
Filtered back-projection theorem

Why machine learning?

There exists a nonlinear Fourier transform adapted to electrical impedance tomography

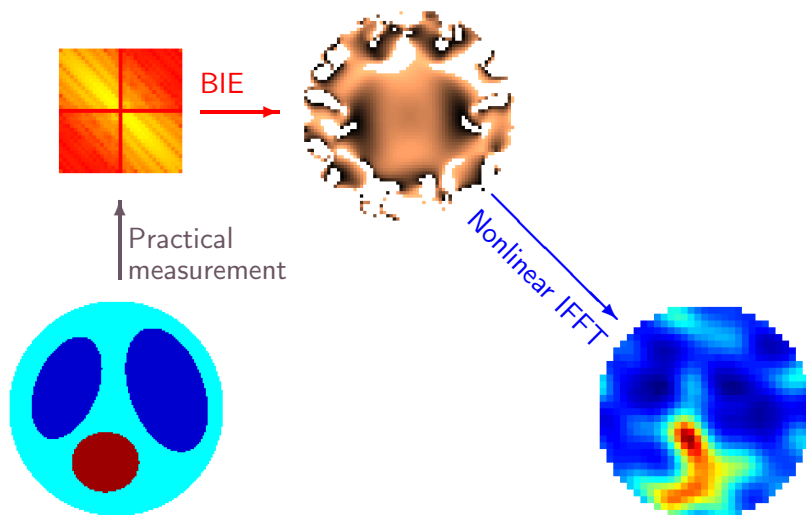


The nonlinear Fourier transform can be recovered from infinite-precision EIT measurements

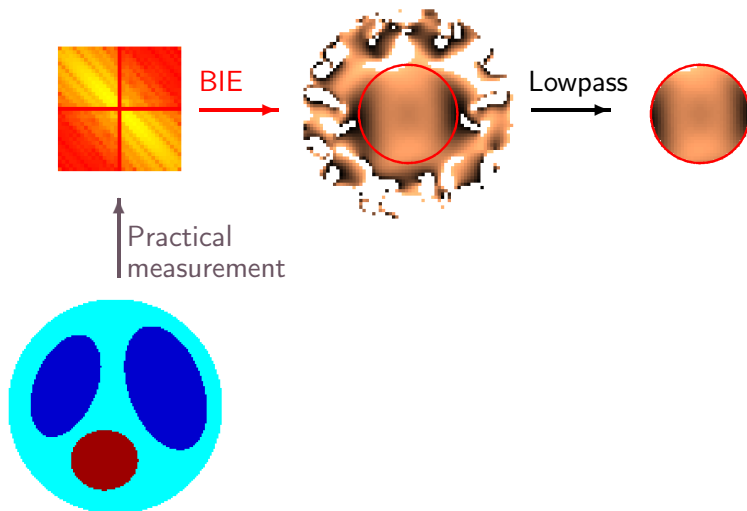


[Nachman 1996]

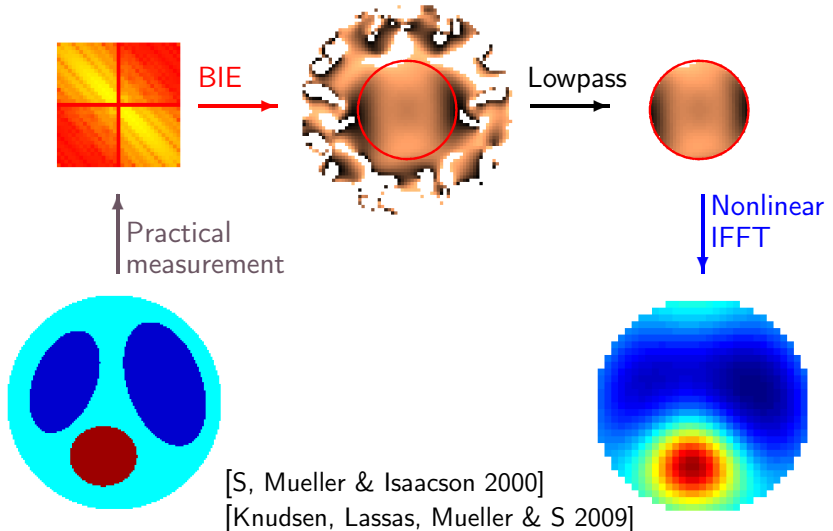
Measurement noise prevents the recovery of the nonlinear Fourier transform at high frequencies



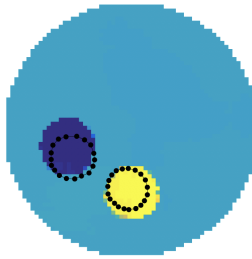
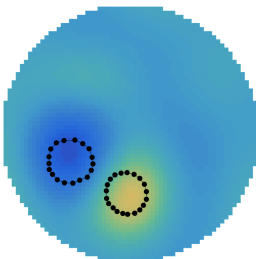
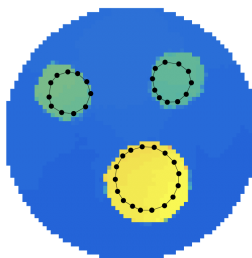
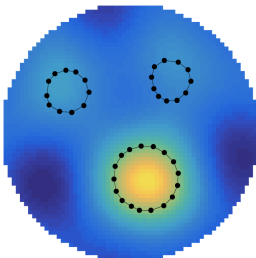
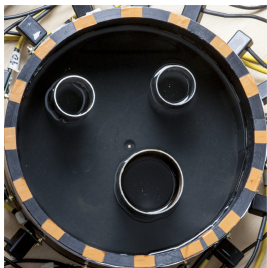
We truncate away the bad part in the transform;
this is a nonlinear low-pass filter



The D-bar method is a regularization strategy for reconstructing the full conductivity distribution



D-bar images can be sharpened by Deep Learning



[Hamilton & Hauptmann 2017]

CGO solutions can serve as nonlinear features in machine learning

<https://www.youtube.com/watch?v=onGMlu7gweg>

[Hamilton, Hauptmann & S 2014]

Outline

Electrical impedance tomography (EIT)

Complex geometric optics (CGO) solutions, D-bar method

Application of EIT to stroke

Virtual Hybrid Edge Detection (VHED)

The scattering series

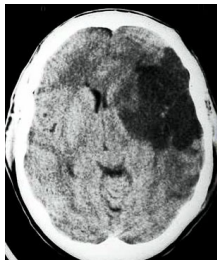
Filtered back-projection theorem

Why machine learning?

Motivation of this study: imaging stroke with EIT

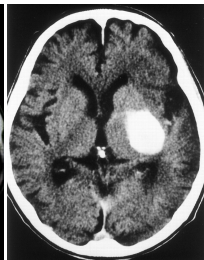
Ischemic stroke:
low conductivity.

CT image from
Jansen 2008



Hemorrhagic stroke:
high conductivity.

CT image from
Nakano *et al.* 2001



Same symptoms in both cases!

Difficulties: resistive skull layer and unknown background. However, see

- Romsauerova, McEwan, Horesh, Yerworth, Bayford & Holder 2006
- Shi, You, Xu, Wang, Fu, Liu & Dong 2009
- Bayford & Tizzard 2012
- Malone, Jehl, Arridge, Betcke & Holder 2014
- Boverman, Kao, Wang, Ashe, Davenport & Amm 2016

Brain EIT imaging is based on covering the head partly by electrodes



Tissue	Ωcm
Cortex	229
White matter	344
Blood	125
CS fluid	69
Scalp	490
Skull	6500

The current activity was initiated by Alex Ross from GE. He is a former student of David Isaacson.

The idea would be to equip every ambulance with an EIT device for classifying strokes



In David Holder's lab at UCL

We have a collaboration network in place for the stroke-EIT project



Project funded for 2017–2020

- Jari Hyttinen & Antti Paldanius (U Tampere)
- Ville Kolehmainen, Asko Hänninen & Jussi Toivanen (U Eastern Finland)
- S, Matti Lassas, Minh Mach & Rashmi Murthy (U Helsinki)

Finnish collaboration:

Stefan Björkman (U Helsinki)
Valentina Candiani (Aalto U)
Antti Hannukainen (Aalto U)
Nuutti Hyvönen (Aalto U)



Nina Forss
Daniel Strbian

International collaboration:

Juan Pablo Agnelli (U Córdoba)
Melody Alsaker (Gonzaga U)
Aynur Çöl (Sinop U)
Sarah Hamilton (Marquette U)
Andreas Hauptmann (UCL)
Jennifer Mueller (CSU),
Toshiaki Yachimura (Tohoku)

The results in this talk are a joint work with

Allan Greenleaf, University of Rochester, NY, USA

Matti Lassas, University of Helsinki, Finland

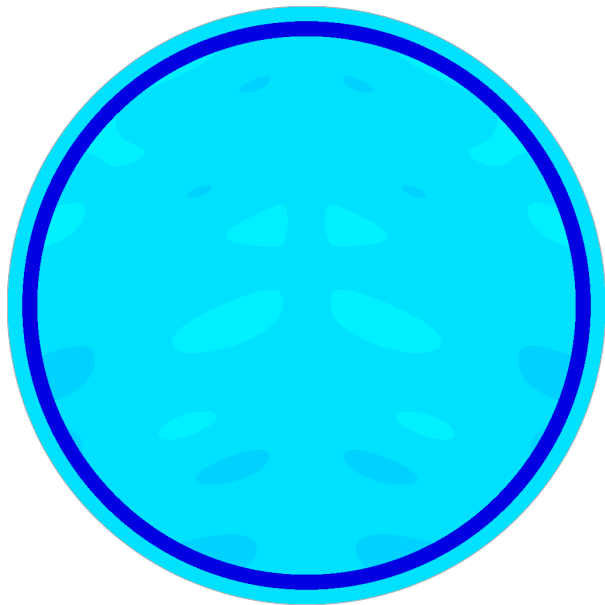
Minh Mach, University of Helsinki, Finland

Matteo Santacesaria, University of Helsinki, Finland

Gunther Uhlmann, University of Washington, USA

Toshiaki Yachimura, Tohoku University, Japan

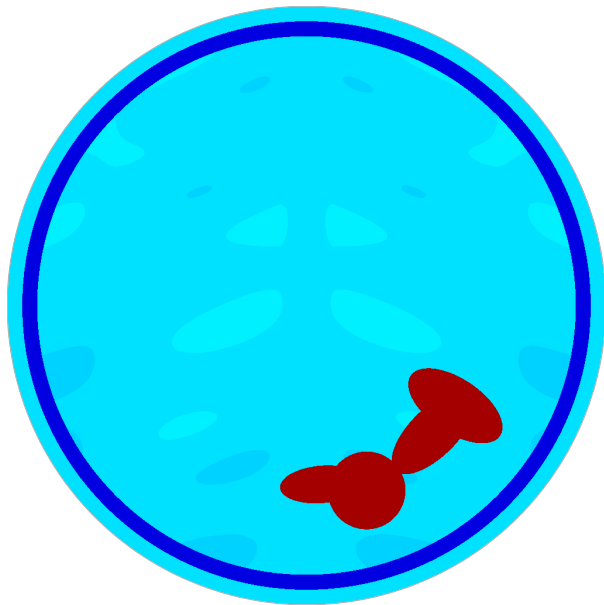
We consider three simulated 2D stroke phantoms:
here healthy brain



We consider three simulated 2D stroke phantoms:
here ischemic stroke



We consider three simulated 2D stroke phantoms:
here hemorrhagic stroke



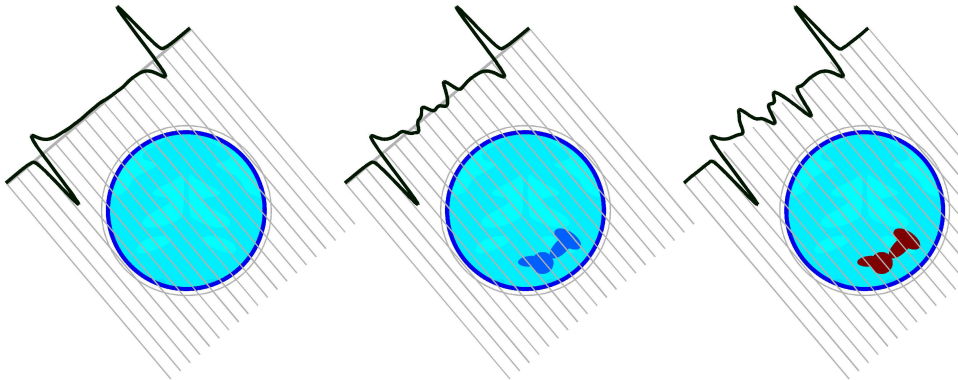
New result: inverse scattering methods can transform EIT into “X-ray tomography”

Video:

<https://www.youtube.com/watch?v=37yOCfBfRJk>

[Greenleaf, Lassas, Santacesaria, S and Uhlmann 2018]

New result: inverse scattering methods can transform EIT into “X-ray tomography”



[Greenleaf, Lassas, Santacesaria, S and Uhlmann 2018]

Outline

Electrical impedance tomography (EIT)

Complex geometric optics (CGO) solutions, D-bar method

Application of EIT to stroke

Virtual Hybrid Edge Detection (VHED)

The scattering series

Filtered back-projection theorem

Why machine learning?

We consider exponentially behaving Complex Geometric Optics (CGO) solutions

Denote $x = (x_1, x_2) \in \mathbb{R}^2$ and $k = i\tau\theta$ where

$$\theta = \theta_1 + i\theta_2 \in \mathbb{C} \quad \text{with } |\theta| = 1.$$

Let $z = x_1 + ix_2 \in \mathbb{C}$ and

$$\eta = \eta_R + i\eta_I = (\theta_1 + i\theta_2, -\theta_2 + i\theta_1) \in \mathbb{C}^2,$$

so that $z\theta = x_1\theta_1 - x_2\theta_2 + i(x_1\theta_2 + x_2\theta_1) = x \cdot \eta$. Note that $\eta \cdot \eta = 0$. We consider solutions of the conductivity equation

$$\nabla \cdot \sigma \nabla u = 0 \quad \text{in } \Omega,$$

with a strictly positive conductivity $\sigma \in L^\infty(\Omega)$, of the form

$$u(x) = e^{i\tau\theta z} w(x, \tau) = e^{i\tau\eta \cdot x} w(x, \tau).$$

Since $u(x) = e^{i\tau\eta \cdot x} w(x, \tau)$ satisfies the conductivity equation,

$$\begin{aligned} 0 &= \frac{1}{\sigma(x)} \nabla \cdot (\sigma(x) \nabla u(x)) \\ &= (\Delta + \frac{1}{\sigma} (\nabla \sigma) \cdot \nabla) (e^{i\tau\eta \cdot x} w(x, \tau)) \\ &= \left(\Delta w(x, \tau) + 2i\tau\eta \cdot \nabla w(x, \tau) + \left(\frac{1}{\sigma} \nabla \sigma \right) \cdot (\nabla + i\tau\eta) w(x, \tau) \right) e^{i\tau\eta \cdot x}. \end{aligned}$$

Hence, we have

$$\Delta w(x, \tau) + 2i\tau\eta \cdot \nabla w(x, \tau) + \left(\frac{1}{\sigma} \nabla \sigma \right) \cdot (\nabla + i\tau\eta) w(x, \tau) = 0.$$

New trick: apply one-dimensional Fourier transform to the complex spectral parameter

Let $\widehat{w}(x, t)$ be the Fourier transform of $w(x, \tau)$ in the τ variable:

$$\widehat{w}(x, t) = \mathcal{F}w(x, t) = \int_{\mathbb{R}} e^{-it\tau} w(x, \tau) d\tau.$$

We call t the *pseudo-time* corresponding to complex frequency τ .
Then equation

$$\Delta w(x, \tau) + 2i\tau\eta \cdot \nabla w(x, \tau) + \left(\frac{1}{\sigma} \nabla \sigma\right) \cdot (\nabla + i\tau\eta) w(x, \tau) = 0$$

yields

$$\Delta \widehat{w}(x, t) + 2\eta \frac{\partial}{\partial t} \cdot \nabla \widehat{w}(x, t) + \left(\frac{1}{\sigma} \nabla \sigma\right) \cdot \left(\nabla + \eta \frac{\partial}{\partial t}\right) \widehat{w}(x, t) = 0.$$

Complex principal type operator leads to singularities propagating along leaves

In the equation

$$\Delta \hat{w}(x, t) - 2\eta \frac{\partial}{\partial t} \cdot \nabla \hat{w}(x, t) + \frac{1}{\sigma} (\nabla \sigma) \cdot (\nabla - \eta \frac{\partial}{\partial t}) \hat{w}(x, t) = 0$$

the principal part is

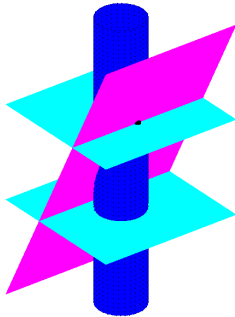
$$\Delta - 2\eta \frac{\partial}{\partial t} \cdot \nabla,$$

which is a **complex principal type operator** in the sense of Duistermaat and Hörmander.

For a **real principal type operator** the characteristic singularities propagate along one-dimensional rays. For instance, for the wave equation the light-like singularities propagate along light rays.

For a **complex principal type operator** the characteristic singularities propagate along two-dimensional surfaces called *leaves*.

We use propagation and reflection of singularities along leaves for detecting inclusions



Here the magenta plane wave hits the blue surface, producing light blue reflected waves.

We use the Beltrami-type complex geometric optics (CGO) solutions

Set $\mu := (1 - \sigma)/(1 + \sigma)$. Write $f = u + iv$ and note that

$$\overline{\partial}_z f_\mu = \mu \overline{\partial}_z \overline{f_\mu} \quad \Leftrightarrow \quad \nabla \cdot \sigma \nabla u = 0 \quad \text{and} \quad \nabla \cdot \sigma^{-1} \nabla v = 0.$$

The CGO solutions of [Astala-Päivärinta 2006] have the form

$$\begin{aligned} f_\mu(z, k) &= e^{ikz}(1 + \omega^+(z, k)), \\ f_{-\mu}(z, k) &= e^{ikz}(1 + \omega^-(z, k)), \end{aligned}$$

with the asymptotic condition

$$\omega^\pm(z, k) = \mathcal{O}\left(\frac{1}{|z|}\right) \text{ as } |z| \rightarrow \infty.$$

Here $ikz = i(k_1 + ik_2)(x + iy)$ and $\overline{\partial}_z = \frac{1}{2}(\partial_x + i\partial_y)$.

This is a brief history of computational solution methods for the Beltrami CGO solutions

1987 Sylvester and Uhlmann: Introduction of CGO solutions

2000 S, Mueller and Isaacson: Numerical CGOs

2006 Astala and Päivärinta: Original Beltrami-type construction

2010 Astala, Mueller, Päivärinta and S:

First numerical solution method

2011 Astala, Mueller, Päivärinta, Perämäki and S:

Novel EIT reconstruction method

2012 Huhtanen and Perämäki:

Preconditioned Krylov subspace method for real-linear systems

2014 Astala, Päivärinta, Reyes and S:

Computational high-frequency experiments

New trick: apply one-dimensional Fourier transform to the complex spectral parameter

In $f_\mu(z, k) = e^{ikz}(1 + \omega^+(z, k))$, write the complex parameter in the form $k = \tau e^{i\varphi}$ with $\tau \in \mathbb{R}$. Denote $\omega^+(z, \tau, e^{i\varphi}) = \omega^+(z, k)$.

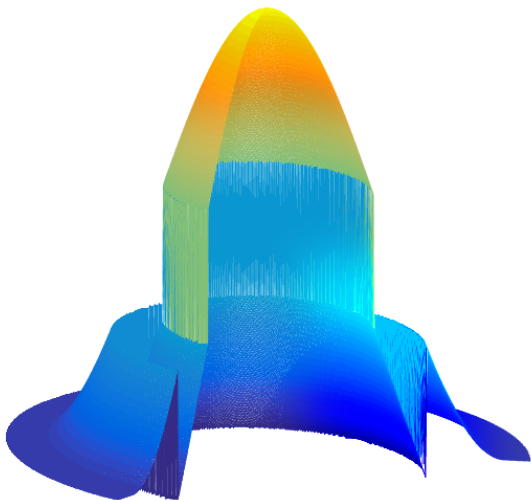
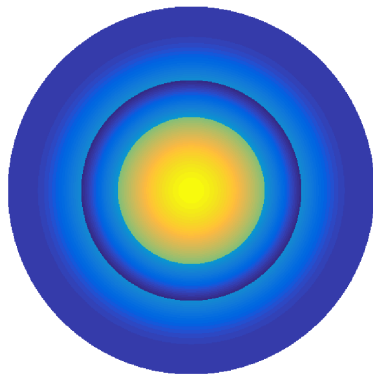
Fourier transform $\omega^+(z, \tau, e^{i\varphi})$ in the τ variable:

$$\widehat{\omega}^+(z, t, e^{i\varphi}) = \mathcal{F}_{\tau \rightarrow t}(\omega^+(z, \tau, e^{i\varphi})) = \int_{-\infty}^{\infty} e^{-it\tau} \omega^+(z, \tau, e^{i\varphi}) d\tau.$$

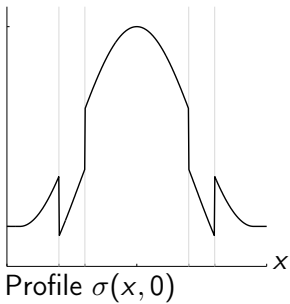
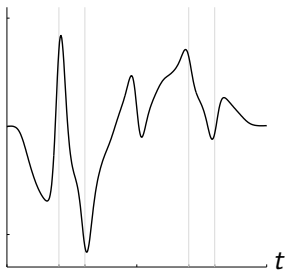
We call t the pseudo-time.

Let us choose a simple rotationally symmetric conductivity for a test case

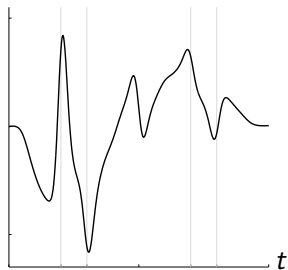
$$\sigma(x, y)$$



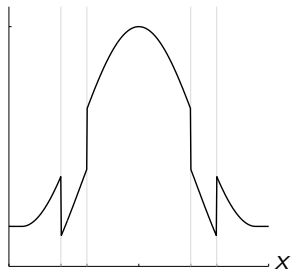
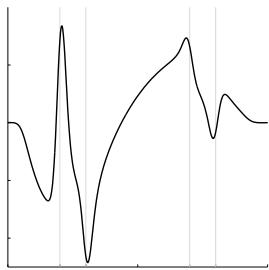
$$\hat{\omega}^+(-1, 2t, 1)$$



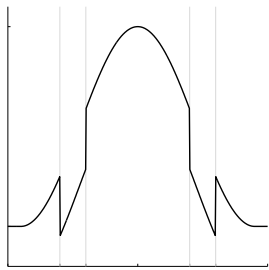
$$\hat{\omega}^+(-1, 2t, 1)$$



$$[\hat{\omega}^+ - \hat{\omega}^-](-1, 2t, 1)$$



Profile $\sigma(x, 0)$



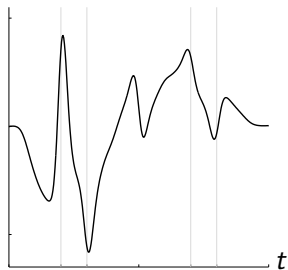
We define an averaging operator

Definition (Greenleaf, Lassas, Santacesaria, S and Uhlmann 2018)

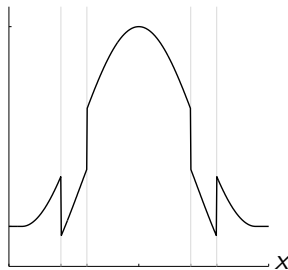
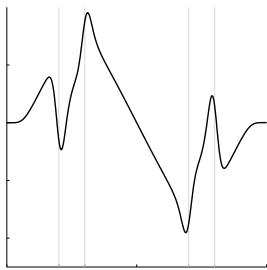
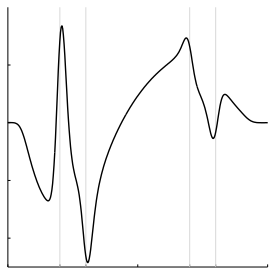
Define operator T^\pm by complex contour integral:

$$T^\pm \mu(t, e^{i\varphi}) = \frac{1}{2\pi} \int_0^{2\pi} \widehat{\omega}^\pm(e^{i\gamma}, t, e^{i\varphi}) e^{i\gamma} d\gamma.$$

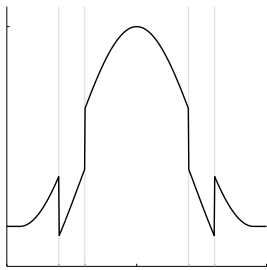
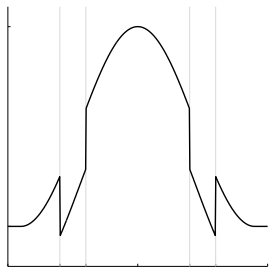
$$\hat{\omega}^+(-1, 2t, 1)$$



$$[\hat{\omega}^+ - \hat{\omega}^-](-1, 2t, 1) \quad [T^+ - T^-]\mu(2t, 1)$$



Profile $\sigma(x, 0)$



Outline

Electrical impedance tomography (EIT)

Complex geometric optics (CGO) solutions, D-bar method

Application of EIT to stroke

Virtual Hybrid Edge Detection (VHED)

The scattering series

Filtered back-projection theorem

Why machine learning?

Cauchy and Beurling transforms

Define the Cauchy and Beurling transforms by

$$Pf(z) = \bar{\partial}^{-1}f(z) = -\frac{1}{\pi} \int_{\mathbb{C}} \frac{f(\lambda)}{\lambda - z} d\lambda_1 d\lambda_2,$$

$$Sg(z) = \partial \bar{\partial}^{-1}g(z) = -\frac{1}{\pi} \lim_{\varepsilon \rightarrow 0} \int_{|\lambda - z| > \varepsilon} \frac{g(\lambda)}{(\lambda - z)^2} d\lambda_1 d\lambda_2.$$

Also, set

$$\begin{aligned}e_k(z) &= \exp(i(kz + \bar{k}\bar{z})), \\ \alpha(z, k) &= -i\bar{k}e_{-k}(z)\mu(z), \\ \nu(z, k) &= e_{-k}(z)\mu(z),\end{aligned}$$

and define the operator A by

$$A := (-\bar{\nu}S - \bar{\alpha}P).$$

We introduce a new scattering series

Huhtanen and Perämäki (2012) modified the original construction of Astala and Päiväranta (2006) for computational purposes. We use the 2012 technique for the construction of a novel scattering series

$$\omega = \sum_{n=1}^{\infty} \omega_n,$$

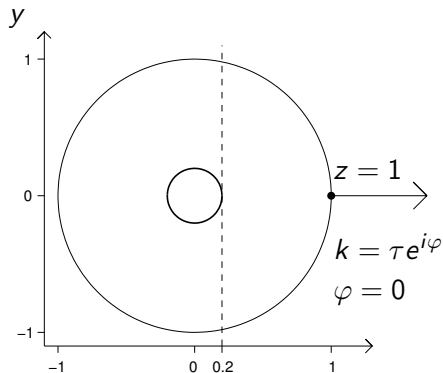
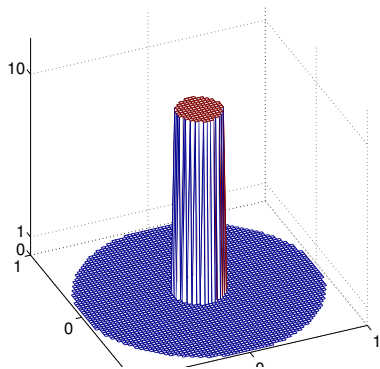
where $A := (-\bar{\nu}S - \bar{\alpha}P)$ and

$$\omega_n = -\bar{\partial}_z^{-1} \overline{u_n}, \quad u_n = -A \overline{u_{n-1}}, \quad u_1 = -\bar{\alpha}.$$

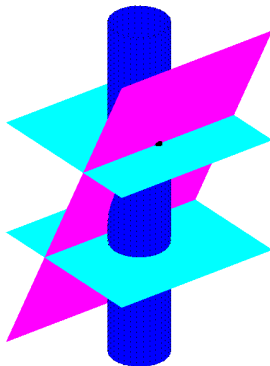
The **single scattering** term $\omega_1 = \bar{\partial}_z^{-1} \alpha$ determines singularities of μ .

The terms ω_n with $n > 1$ arise from **multiple scattering**.

Let us consider a rotationally symmetric conductivity with jump along the circle $|z| = 0.2$

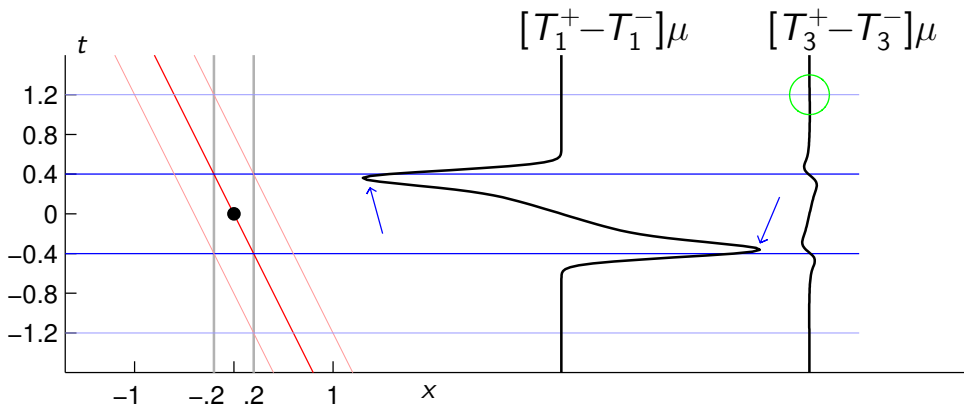


We use propagation and reflection of singularities along leaves for detecting inclusions

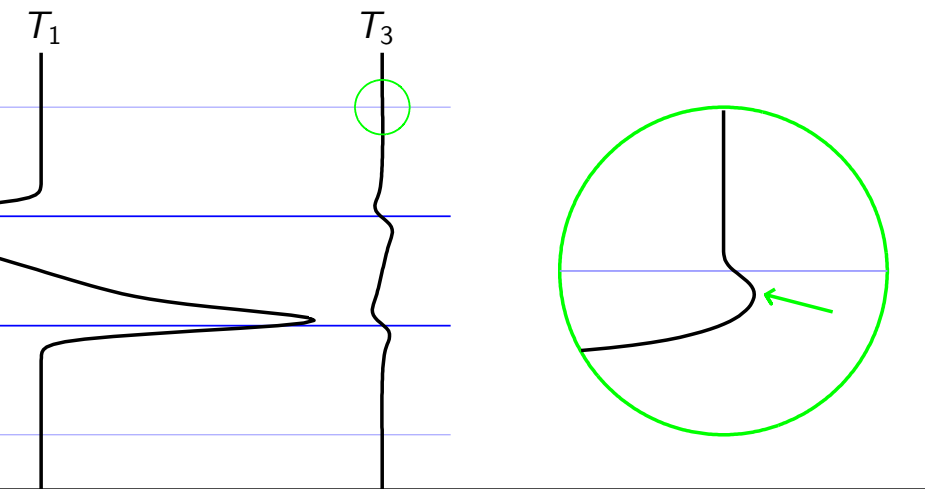


Here the magenta plane wave hits the blue surface, producing light blue reflected waves.

Here are the two lowest-order odd terms
in the scattering series, with subtraction



Detail from the previous slide, with 70-fold magnification of the function inside green circle



Outline

Electrical impedance tomography (EIT)

Complex geometric optics (CGO) solutions, D-bar method

Application of EIT to stroke

Virtual Hybrid Edge Detection (VHED)

The scattering series

Filtered back-projection theorem

Why machine learning?

Recovery by complex “filtered back-projection”

Theorem. (Greenleaf, Lassas, Santacesaria, S and Uhlmann 2018)

Define averaged operators T_j^\pm for $j = 1, 2, 3, \dots$ by the complex contour integral:

$$T_j^\pm \mu(t, e^{i\varphi}) = \frac{1}{2\pi i} \int_{\partial\Omega} \widehat{\omega}_j^\pm(z, t, e^{i\varphi}) dz,$$

Then we have a filtered back-projection formula

$$(-\Delta)^{-1/2} (T_1^\pm)^* T_1^\pm \mu = \mu.$$

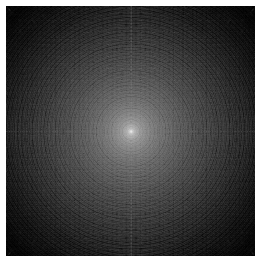
Simple example of tomographic imaging with a double-disc target

<https://youtu.be/5DUGTXd26nA>

We can back-project the measured data into the image, integrating over all directions

<https://youtu.be/5DUGTXd26nA>

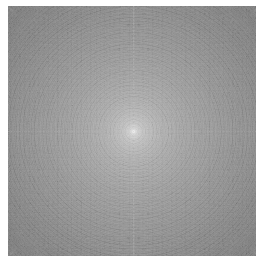
Final FBP reconstruction involves filtering on top of the back-projection



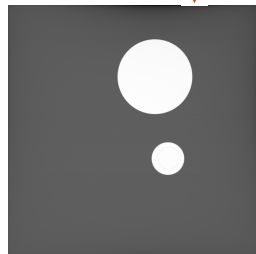
↑ FFT



Multiplication by $|\xi|$
(Calderón's operator)



IFFT ↓



FBP-type reconstruction algorithm for EIT

Step 1. Given the measurement Λ_σ , follow

[Astala, Mueller, Päiväranta, Perämäki & S 2011]

to compute both $\omega^+(x, k)$ and $\omega^-(x, k)$ for $x \in \partial\Omega$ by solving the boundary integral equation derived in [Astala & Päiväranta 2006].

Note: In practice this can only be done in a disc $|k| < R$ with R depending on measurement noise amplitude.

Step 2. Write $k = \tau e^{i\varphi}$ and compute the partial Fourier transform to get $\hat{\omega}^\pm(z, t, e^{i\varphi})$.

Note: In practice the Fourier transform needs to be windowed.

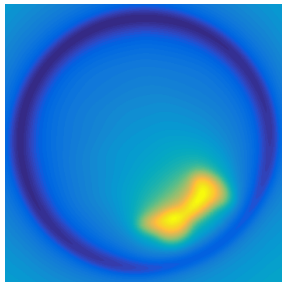
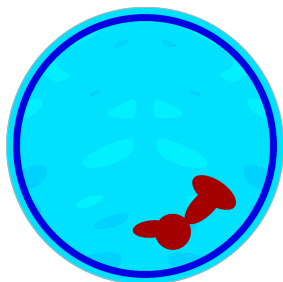
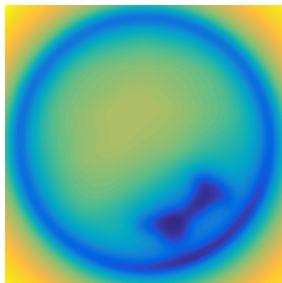
Step 3. Reconstruct $\sigma = (\mu - 1)/(\mu + 1)$ approximately as $(\tilde{\mu} - 1)/(\tilde{\mu} + 1)$ using formula $\tilde{\mu} = (\tilde{\mu}^+ - \tilde{\mu}^-)/2$ with

$$\tilde{\mu}^\pm := \Delta^{-1/2} (T_1^\pm)^* T^\pm \mu.$$

Conductivity



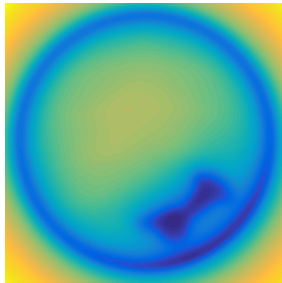
Filtered back-projection



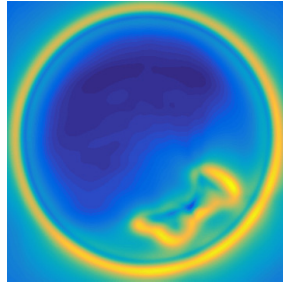
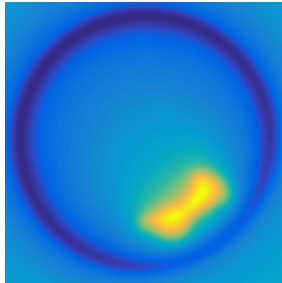
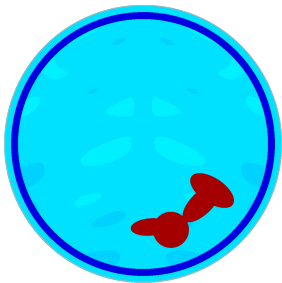
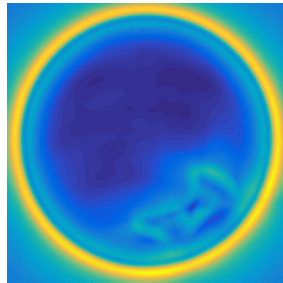
Conductivity



Filtered back-projection



" Λ -tomography"



Outline

Electrical impedance tomography (EIT)

Complex geometric optics (CGO) solutions, D-bar method

Application of EIT to stroke

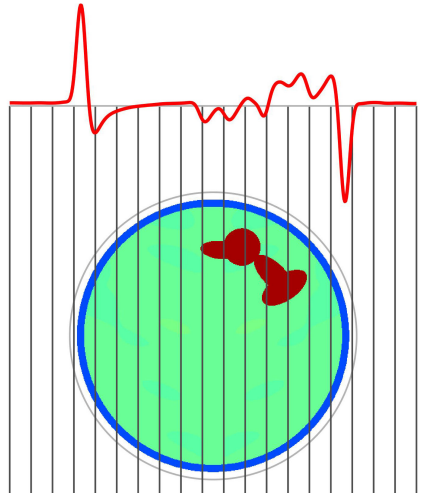
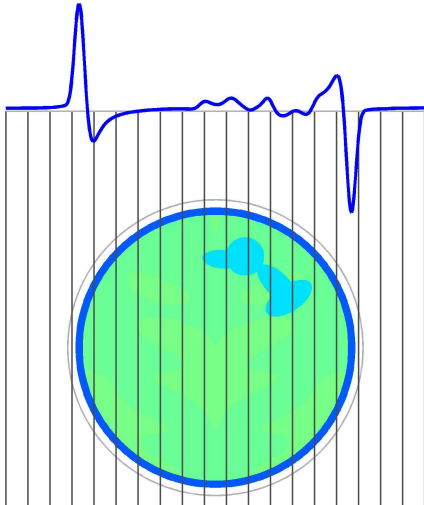
Virtual Hybrid Edge Detection (VHED)

The scattering series

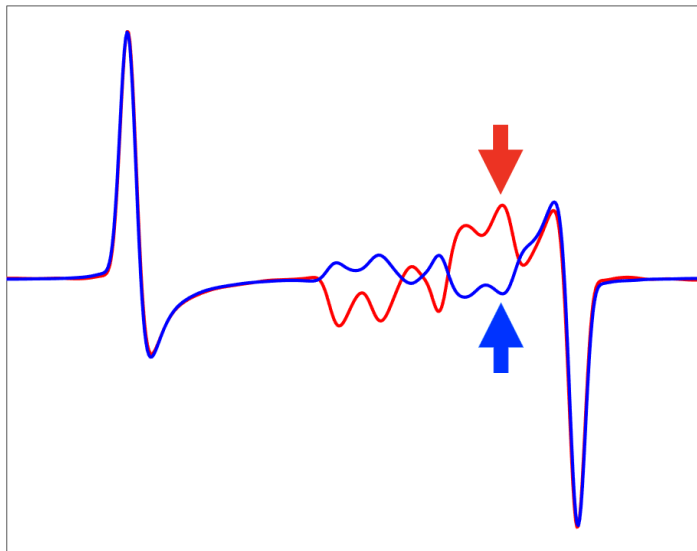
Filtered back-projection theorem

Why machine learning?

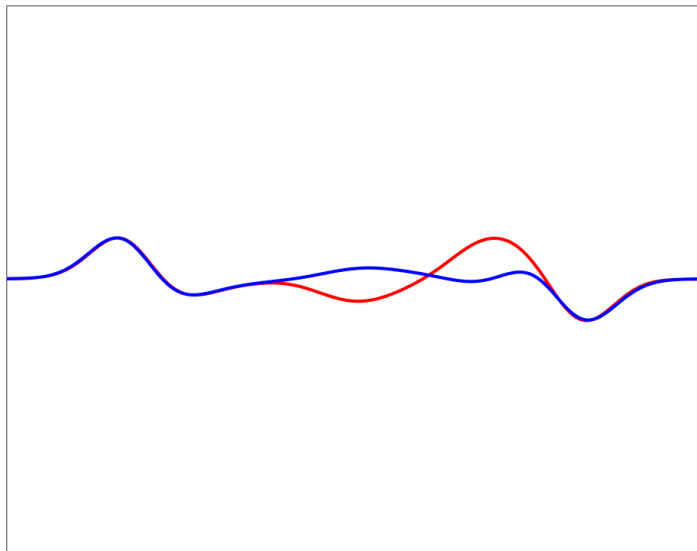
We can see the difference in conductivity reflected in the VHED projections (blue and red graphs)

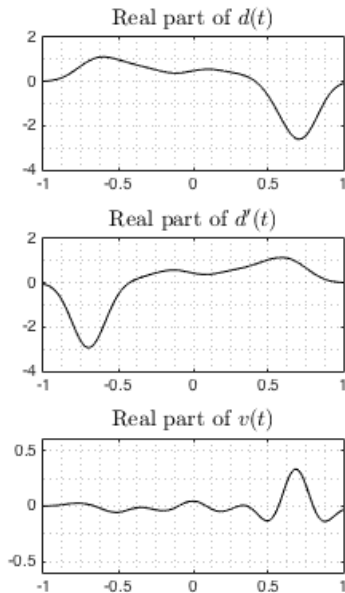
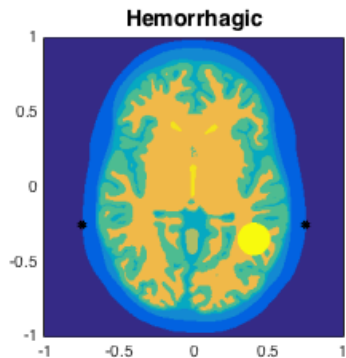


Given unrealistic-precision EIT measurements on full boundary we can classify the stroke easily

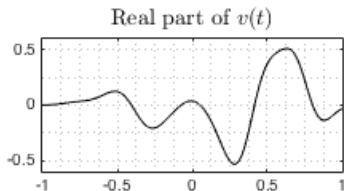
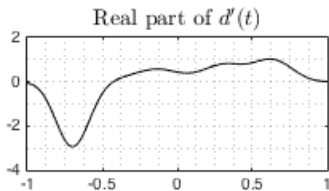
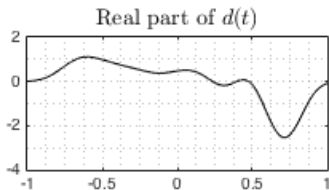
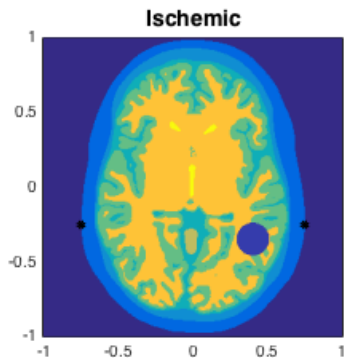


Practical EIT measurements blur the information due to heavily windowed Fourier transform





Simulations by Antti Hannukainen and Minh Mach



Simulations by Antti Hannukainen and Minh Mach

Practical problems in applying VHED

VHED works with ideal simulated data and simple digital phantoms. However, these issues must be solved before it can be applied to stroke classification:

Data is noisy. We know the Fourier transform of the desired function only in an interval $[-R, R]$ with $R \approx 4$.

Anatomy is complicated. Need to be test with realistic phantoms.

We can only measure on a part of the boundary. Some progress is reported in [Hauptmann, Santacesaria and S 2017].

Measurements are done using a finite number of electrodes.
Recovering CGO solutions from electrode data needs new research.

People are three-dimensional. VHED needs to be extended to 3D.

Thank you for your attention!



This project started in 2000

